# Effect of $H_2O$ on the Diffusion of $N_2$ in PMMA: A Molecular Dynamics Simulation Study

**R. K. Bharadwaj**

*Avery Research Center, 2900 Bradley Street,*
*Pasadena, California 91107*

*Received March 7, 2002*
*Revised Manuscript Received April 17, 2002*

## Introduction

The study of gas diffusion in polymeric matrices holds tremendous technological importance in the design of barrier and membrane materials.[1] Insofar, most diffusion studies in the literature, both experimental[1] and simulations,[2] have exclusively addressed the diffusion of a single penetrant species in a polymeric matrix. In contrast, little is known about the effect of another species on the diffusing characteristics of a penetrant, even in the small molecule limit.[1,3−5] A copenetrant, depending on its concentration and chemical interactions with the polymer, could lead to plasticization of the polymer matrix and also have an effect on thermodynamic solubility of another species.[1] In this regard, $H_2O$ as a copenetrant species is particularly important since it is sorbed in many polymers, albeit to varying concentrations. It is therefore of fundamental interest to develop an understanding of the diffusion of small gases in the presence of $H_2O$. It is recognized that the effect of other similar codiffusing small molecule pentrants is also important in order to develop a detailed mechanistic picture. There are polymeric materials that have the ability to absorb rather large amounts of $H_2O$, such as poly(vinyl alcohol) and poly(ethylene vinyl alcohol), which are excellent barriers to the diffusion of air under dry conditions but degrade rapidly with increasing $H_2O$ content, where the effect has been well studied.[6,7] The effect on other polar polymers such as acrylics, nylons, etc., that are capable of aborbing limited quantities of $H_2O$ is less clear. In addition, $H_2O$ as a copenetrant holds special importance, in that, it is perhaps the only small molecule penetrant that is capable of hydrogen bonding with polar polymers that are capable of forming such bonds. The precise manner in which the $H_2O$ molecules are incorporated in the matrix (clusters vs randomly distributed) and the interactions with the polymer could change the packing and thermodynamic properties to affect the diffusive characteristics of a gas molecule.

The present work involves the use of molecular dynamics simulations to predict the transport properties of $N_2$ in PMMA as a function of $H_2O$ concentration. PMMA was chosen as the polymeric system of choice given that the polymer is polar and absorbs $H_2O$ under ordinary conditions and is a prototypical glassy polymeric system. PMMA absorbs ∼1.7 wt % of $H_2O$ at saturation and room temperature conditions.[8] The mechanism of sorption was found consistent with the dual-mode sorption model, where between 40 and 60% of the $H_2O$ molecules are accommodated in the free volume (with no overall volumetric change) and remaining taken up by a swelling process.[8−10] The glass transition temperature decreases by ∼20 K in the saturation limit.[11] In this concentration regime, the mechanical properties are also found to degrade rapidly affecting the fatigue performance, modulus, and crazing stress.[12,13] From the perspective of diffusion of another species in the presence of $H_2O$, it is clear that the reduction in the $T_g$ and the dual-mode sorption behavior could dramatically impact the available free volume and chain dynamics accompanying the diffusive process.

## Simulation Details

All simulations were performed using the Cerius2 software.[14] The Discover module was used to perform the molecular dynamics simulations using the Compass force field parameters. A single PMMA chain consisting of 100 methyl methacrylate monomers in the syndiotactic configuration was constructed and packed into a cubic simulation cell at a density of 0.8 g $cm^{-3}$. The simulation cell was subsequently minimized to relax the unfavorable overlaps and subjected to *NPT* simulations (constant particle number, pressure, and temperature) using the Andersen and Berendsen methods to control $T$ and $P$, respectively. A time step of 1 fs was used to integrate the equations of motion, and a cutoff radius of 9.5 Å was used to truncate the nonbonded van der Waals and electrostatic interactions. The electrostatic interactions were treated using group-based cutoffs. The PMMA system was initially subjected to 500 ps of *NPT* dynamics at 560 K and 1 atm to equilibrate the system. The systems at lower temperatures (530 and 500 K) were prepared by using the equilibrated configuration of the preceding higher temperature using 500 ps of *NPT* dynamics. The specific volume was observed to fluctuate about a well-defined mean over the time scale of the dynamics, indicating that the equilibrium density for the given temperature and pressure had been attained.

Diffusion of a single $N_2$ penetrant in the PMMA matrix was studied as a function of $H_2O$ concentration at three different temperatures (500, 530, and 560 K). Four concentrations of $H_2O$ were studied 0, 0.9, 3.5, and 8.2 wt % corresponding to 0, 5, 20, and 50 $H_2O$ molecules per simulation cell. The $N_2$ and $H_2O$ molecules were inserted at random locations in the simulation cell initially built at the time averaged density derived for pure PMMA as predicted from *NPT* simulations. Subsequently, *NPT* dynamics were conducted on these systems to reequilibrate and predict the densities as a function of concentration and temperature for a period of 300 ps. The resulting equilibrated configurations at the correct time averaged density appropriate for the temperature and $H_2O$ concentration were used to initiate *NVT* (constant particle number, volume, and temperature) dynamics for a period of 1 ns.

## Results and Discussion

The time-averaged density of the PMMA systems at four different $H_2O$ concentrations and three different temperatures as obtained from *NPT* simulations are shown in Figure 1. As expected, the density of PMMA decreases with increasing $H_2O$ concentration. We note that at 0.9 wt % of $H_2O$ the density is nearly identical to that of pure PMMA.

10.1021/ma020342k CCC: \$22.00

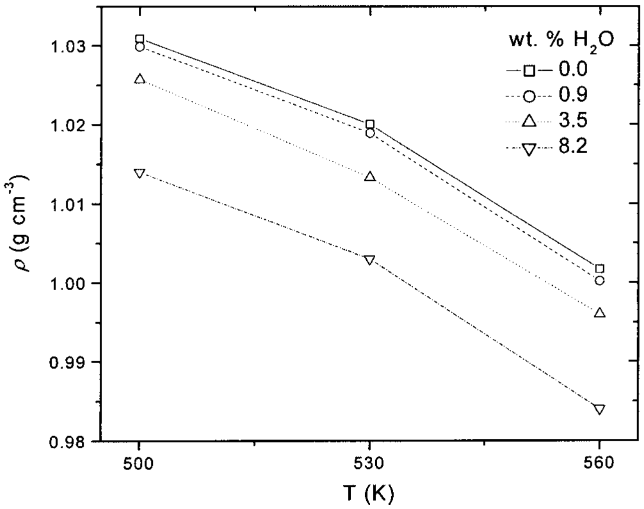

**Figure 1.** Time-averaged densities for PMMA determined from NPT-MD simulations as a function of temperature at several different concentrations of $H_2O$.

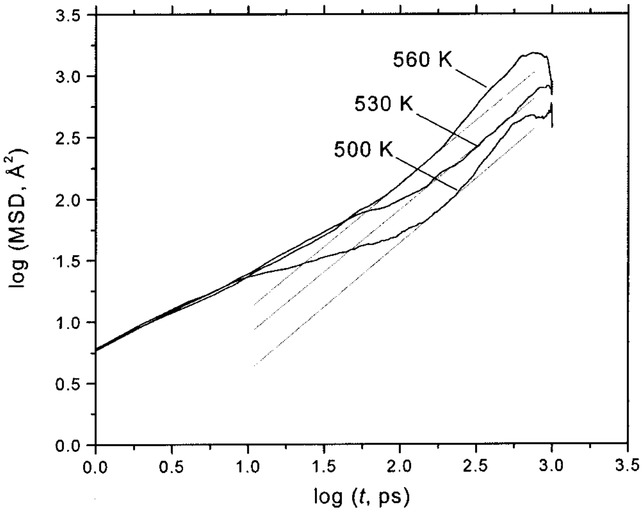

**Figure 2.** Log−log plot of mean-squared displacement vs time for $N_2$ in syndiotactic PMMA at 500, 530, and 560 K. The lines represent slope = 1 fits to the true diffusion regime.

The self-diffusion coefficient ($D$) of $N_2$ was computed using the Einstein equation, which in the long time limit is given by $\{\langle|r_i(0) - r_i(t)|^2 = 6Dt\}$, where $r$ represents the position coordinate of the penetrant $i$ as a function of time $t$. The angular brackets represent ensemble and time averaging of the trajectory. The above equation correctly yields the diffusion coefficient provided a sufficient number of diffusive events have occurred to yield a true Fickian process. In practice, the unbound position coordinate of the diffusing $N_2$ molecule was saved every 1 ps of a 1000 ps simulation trajectory, and the mean-squared displacement was calculated using the above expression. The practice of initiating the calculation from multiple time origins spaced 1 ps apart was used to improve statistics. Typical behavior of the mean-squared displacement vs time is shown in a log−log plot for $N_2$ in pure PMMA in Figure 2.

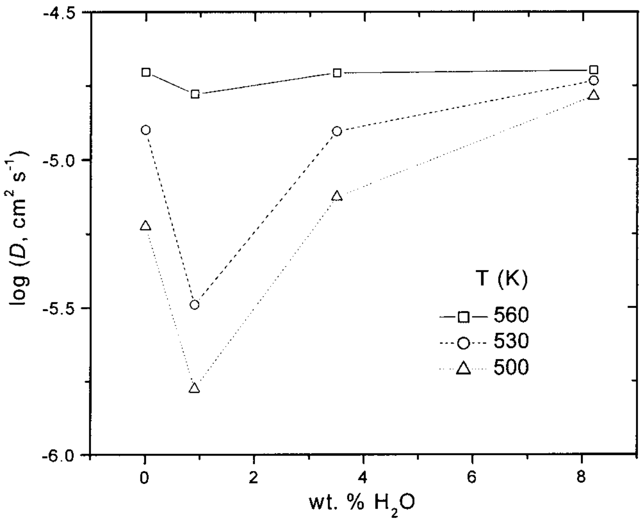

**Figure 3.** Dependence of the diffusion coefficient of $N_2$ on $H_2O$ concentration in PMMA from MD simulations at three temperatures.

**Table 1. Diffusion Coefficients ($D$ in cm$^2$ s$^{-1}$) for $N_2$ as a Function of $H_2O$ Concentration and Temperature; the Fractional Free Volume (ffv) for the Systems at 500 K Is Also Shown**

| wt % $H_2O$ | 0.0 | 0.9 | 3.5 | 8.2 |
|---|---|---|---|---|
| $D$ (560 K) | 1.97E−5[a] | 1.66E−5 | 1.96E−5 | 1.99E−5 |
| $D$ (530 K) | 1.26E−5 | 3.23E−6 | 1.24E−5 | 1.84E−5 |
| $D$ (500 K) | 5.97E−6 | 1.67E−6 | 7.49E−6 | 1.63E−5 |
| ffv (500 K) | 0.425 | 0.420 | 0.431 | 0.461 |

[a] Read as 1.97 × $10^{-5}$.

Three regions may be clearly discerned from the above curves. At short times, the diffusion is anomalous in that the slope of the curve is much less than 1 and represents the *cage effect* where the penetrant spends a great deal of time sampling a local free volume in the matrix. At longer time scales, once the penetrant has executed hops over several free volume sites, the diffusion approaches Fickian behavior with slope equaling 1. This region, representing the true diffusion regime, occurs at all temperatures over a significant time period in Figure 2, indicating that the original trajectory was long enough to capture the diffusive process, yielding a reliable estimate of the diffusion coefficient. Toward the end of the trajectory, the curves become increasingly noisy given that there are fewer origins available for averaging. The intercept of the slope = 1 linear fit to each of the above curves corresponds to log(6$D$), thereby yielding the diffusion coefficient.

The self-diffusion coefficient for $N_2$ in PMMA was computed in a similar fashion for systems with different concentrations of $H_2O$ molecules and is shown in Figure 3 and summarized in Table 1. The most striking feature of the concentration dependence of the diffusion coefficient shown in Figure 3 is the presence of a minimum at all three temperatures studied. That is, the diffusion of $N_2$ is retarded in the presence of small quantities of $H_2O$. As the concentration of $H_2O$ increases beyond ~2.0 wt %, the diffusion coefficient increases, approaching and exceeding the value observed for the pure PMMA case. The effect is more pronounced at 500 and 530 K than at 560 K.

It is instructive to analyze the static free volumes in the PMMA systems as a function of $H_2O$ concentration. The static fractional free volume was calculated by inserting a large number of points at random in many simulation configurations corresponding to a given temperature and $H_2O$ concentration.[15] Subsequently, the distance of every atom center from the inserted point was computed, and the minimum distance and the corresponding atom center were recorded. If the distance was smaller than the van der Waals radius of the closest

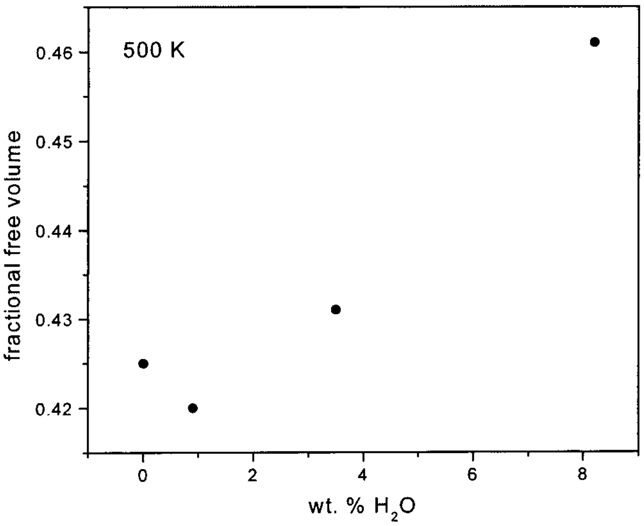

**Figure 4.** Fractional free volume vs $H_2O$ concentration in PMMA at 500 K.

atom, it was considered to lie in occupied volume. If the distance was greater than the van der Waals radius of the closest atom, then the largest sphere that could be placed at that point was computed. The fraction of all points lying in unoccupied space yields the fractional free volume for a given sphere radius. Thus, a distribution of the fractional free volume corresponding to a given sphere radius obtains. Extrapolation of the fractional free volume to zero sphere radius yields the total free volume in the system. The fractional free volume available in the PMMA systems is plotted as a function of the $H_2O$ concentration in Figure 4 at 500 K. As seen, the fractional free volume mimics the behavior seen in the $N_2$ diffusivity. At low $H_2O$ concentrations, there appears to be a net decrease in the fractional free volume. With increasing $H_2O$ concentration, the fractional free volume is observed to increase up to and beyond that available in the pure polymer. Recall that the decrease in density in going from 0 to 0.9 wt % $H_2O$ was negligible, indicating that the decrease in fractional free volume is particularly severe since it is not accompanied by matrix swelling. At low concentrations, $H_2O$ molecules appear to be accommodated in the available free volume in the PMMA matrix, resulting in a decrease in the free volume available to a diffusing penetrant. As the concentration of $H_2O$ is increased, the volumetric swelling of the polymer matrix occurs, increasing the available free volume leading to a net increase in the diffusivity of $N_2$. This behavior is consistent with available experimental data for the sorption behavior of $H_2O$ in PMMA.[8,9] From sorption experiments, it is known that PMMA sorbs moisture in accordance with the dual-mode sorption mechanism. That is, a fraction of the $H_2O$ molecules are accommodated in the PMMA matrix without resulting in a volumetric change. As the concentration is increased, new $H_2O$ molecules can no longer be accommodated in the free volume, which is saturated and therefore leads to swelling of the matrix. The static free volume data presented here support this observation. It is to be noted that the plasticization effect of the $H_2O$ molecules on the PMMA matrix leads to a decrease in the $T_g$, enhancing the chain dynamics, which could also help enhance the diffusion at higher concentrations. It is known from experiments that the $T_g$ decreases by $\sim$20 K at $\sim$1.9% $H_2O$ content in PMMA.[11] This implies increased chain mobilities with increasing $H_2O$ content, and there is a contribution from this factor aside from the increase in the static free volume. Nevertheless, we can conclude that, at the low concentrations of sorbed $H_2O$, the decrease in the static free volume appears to correlate well with the observed trend in the $N_2$ diffusivity. Further work is required in exploring this phenomenon in different glassy polymeric matrices with different combinations of copenetrants to comment on the generality of these findings.

**Acknowledgment.** The author thanks Drs. R. Mehrabi and K. Christodoulou for bringing this topic to his attention and for numerous stimulating discussions.

## References and Notes

(1) Stannett, V. In *Diffusion in Polymers*; Crank, J., Park, G. S., Eds.; Academic Press: New York, 1968; p 41.
(2) Theodorou, D. N. In *Diffusion in Polymers*; Neogi, P., Ed.; Marcel Dekker: New York, 1996; p 67.
(3) Poulsen, L.; Ogilby, P. R. *J. Phys. Chem. A* **2000**, *104*, 2573.
(4) Wang, B.; Ogilby, P. R. *Can. J. Chem.* **1995**, *73*, 1831.
(5) Dhingra, S. S.; Marand, E. *J. Membr. Sci.* **1998**, *141*, 45.
(6) *Polymer Permeability*; Cornyn, J., Ed.; Elsevier: London, 1985.
(7) Samus, M. A.; Rossi, G. *Macromolecules* **1996**, *29*, 2275.
(8) Turner, D. T. *Polymer* **1982**, *23*, 197.
(9) Drotning, W. D.; Roth, E. P. *J. Mater. Sci.* **1989**, *24*, 3137.
(10) Masi, P.; Nicodemo, L.; Migliaresi, C.; Nicolais, L. *Polym. Commun.* **1984**, *25*, 331.
(11) Smith, L. S. A.; Schmitz, V. *Polymer* **1988**, *29*, 1871.
(12) Smith, L. S. A.; Sauer, J. A. *Plastics Rubber Proc. Appl.* **1986**, *6*, 57.
(13) Chen, C. C.; Shen, J.; Sauer, J. A. *Polymer* **1985**, *26*, 89.
(14) *Cerius2* 4.6; Accelrys Inc.: San Diego, CA, 2001.
(15) Bharadwaj, R. K.; Boyd, R. H. *Polymer* **1999**, *40*, 4229.

MA020342K